J Mater Sci (2009) 44:6069–6077
DOI 10.1007/s10853-009-3838-4

Optical characterization of a new donor–acceptor type conjugated polymer derived from 3,4-diphenylthiophene

M. G. Manjunatha · Airody Vasudeva Adhikari · Pramod Kumar Hegde · C. S. Suchand Sandeep · Reji Philip

Received: 23 June 2009 / Accepted: 21 August 2009 / Published online: 4 September 2009

Abstract A new donor–acceptor type poly{2-(3,4-didecyloxythiophen-2-yl)-5-[3,4-diphenyl-5-(1,3,4-oxadiazol-2-yl) thiophen-2-yl]-1,3,4-oxadiazole} (**P1**) has been designed and synthesized starting from thiodiglycolic acid, 1,2-diphenylethane-1,2-dione, and diethyl oxalate through multi-step reactions using precursor polyhydrazide route. The charge-transporting and linear optical property of the polymer has been investigated by cyclic voltammetric, UV–visible, and fluorescence emission spectroscopic studies. The UV–visible absorption spectrum of polymer in thin film form showed maxima at 420 nm. The polymer displayed bluish-green fluorescence both in solution and thin film form. The optical band gap is determined to be 2.27 eV. Third-order nonlinear optical property of the new polymer has been investigated at 532 nm using single beam Z-scan and degenerate four wave mixing (DFWM) techniques with nanosecond laser pulses. The absorptive nonlinearity observed for the polymer **P1** is of optical limiting type, which arises due to an "effective" three-photon absorption (3PA) process. The third-order nonlinear optical susceptibility ($\chi^{(3)}$) of the polymer is found to be 0.831×10^{-12} esu. Both linear and nonlinear optical studies revealed that the new polymer (**P1**) is a promising material for applications in photonic devices.

M. G. Manjunatha · A. V. Adhikari (✉) · P. K. Hegde
Organic Chemistry Division, Department of Chemistry, National Institute of Technology Karnataka, Surathkal, Mangalore 575025, India
e-mail: avchem@nitk.ac.in; avadhikari123@yahoo.co.in

C. S. Suchand Sandeep · R. Philip
Light and Matter Physics Group, Raman Research Institute, Sadashiva Nagar, Bangalore 560080, India

Introduction

Materials exhibiting strong nonlinear optical (NLO) properties have received considerable attention due to their potential applications in optical communications, optical switching, optical data storage, and eye and sensor protection [1–3]. From NLO studies conducted in several media, organic materials have turned out to be attractive mainly due to their versatility, high nonlinearity, ultra-fast response, and the flexibility in tuning the optical properties. Recently, conjugated polymeric systems have emerged as a promising class of NLO materials, characterized by large third-order susceptibility along the directions of polymer chain. These macromolecules offer good flexibility at both molecular and bulk levels so that structural modifications necessary to optimize them for specific device applications are possible. As the nonlinear response of these systems is determined primarily by their chemical structure, one can design unique molecular structures and synthesize compounds with enhanced nonlinear response by introducing suitable substituent groups.

In general, if there is a presence of strong π-electron delocalization in the molecular structure, the NLO properties will be enhanced. Recently, Cassano et al. [4] had reported a new strategy for tuning the linear and nonlinear optical properties of conjugated polymers. According to them, incorporation of alternate electron-acceptor and electron-donor units in the polymer backbone would enhance the NLO properties, mainly due to hyperpolarizability.

Apart from NLO, conjugated polymers find applications in devices as well, such as in light emitting diodes (LEDs), field effect transistors, electrochemical cells, and organic photovoltaic cells. The newly developed polymers, poly (1,4-phenylenevinylene) (PPV) [5], poly(*p*-phenylene) (PPs)

[6], polyfluorenes (PFs) [7], and polythiophenes (PTs) [8] were in the focus of such investigations recently.

The third-order optical nonlinearity of thiophene based polymers is currently under investigation mainly because of their chemical stability, easy processibility, and readiness of functionalities [9–11]. Good film forming properties, solubility, and adequate mechanical properties have made them better choices for device fabrication in comparison with their inorganic counterparts. For example, nonlinear optical properties can be synthetically tuned in polythiophenes by introducing electron releasing and electron accepting segments in the polymer chain, which would result in increased delocalization in the molecule. Following a similar strategy, John Kiran and coworkers studied the relationship between the structure and NLO properties of few donor–acceptor type thiophene based conjugated polymers. It was found that electron releasing and electron accepting groups along the polymer backbone would be a promising molecular design for enhancing the third-order NLO properties [12].

In this context, it has been planned to incorporate 3,4-diphenylthiophene moiety in between 3,4-dialkoxy substituted thiophenyl oxadiazole donor–acceptor type systems in our synthetic design, in order to enhance the conjugation within the polymer chain, with the expectation that the resulting molecule would exhibit better NLO properties. Further, it has been predicted that the presence of 3,4-diphenyl thiophene units will reduce the steric repulsion between the bulky alkyl groups and increase the planarity of the polymer chain. In this communication, we hereby report the synthesis of hitherto unknown polymer carrying {2-(3,4-didecyloxythiophen-2-yl)-5-[3,4-diphenyl-5-(1,3,4-oxadiazol-2-yl)thiophen -2-yl]-1,3,4-oxadiazole}unit and the investigation of their optical properties in detail.

Experimental

Materials

3,4-Didecyloxythiophene-2,5-dicarbohydrazide (**4**) was synthesized according to the reported procedure [13]. 3,4-Diphenylthiophene-2,5-dicarboxylic acid (**2**) was synthesized according to the reported procedure [14]. Dimethylformamide and acetonitrile were dried over CaH_2. Thiodiglycolic acid, 1,2-diphenylethane-1,2-dione (benzil), tetrabutylammoniumperchlorate (TBAPC), and *n*-bromodecane were purchased from Lanchaster (UK) and were used as received. All the solvents and reagents were of analytical grade. They were purchased commercially and used without further purification.

Instrumentation

Infrared spectra of all intermediate compounds and polymers were recorded on a Nicolet Avatar 5700 FTIR (Thermo Electron Corporation). The UV–visible and fluorescence emission spectra were measured in Perkin Elmer Lambda-750 UV–visible and Jasco FP 6200 spectrofluorimeter, respectively. ^{1}H NMR spectra were obtained with AMX 400 MHz FT-NMR spectrophotometer using TMS/solvent signal as internal reference. Mass spectrum was recorded on a Jeol SX-102 (FAB) Mass Spectrometer. Elemental analyses were performed on a Flash EA1112 CHNS analyzer (Thermo Electron Corporation). The thermal stability of the polymer was analyzed by SII-EXSTAR6000TG/DTA6300 Thermo Gravimetric Analyzer (TGA). The electrochemical studies of the polymers were carried out using a AUTOLAB PGSTAT30 electrochemical analyzer. Cyclic voltammograms were recorded using a three-electrode cell system, with glassy carbon button as working electrode, a platinum wire as counter electrode and an Ag/Ag^+ electrode as the reference electrode. Molecular weight of the polymer was determined on Waters make gel permeation chromatography (GPC) using polystyrene standards in THF solvent.

Z-scan measurement

The Z-scan technique developed by Sheik Bahae et al. [15] is widely used for measuring the nonlinear absorption coefficient and nonlinear refractive index of materials. In the "open aperture" Z-scan, which gives information about the nonlinear absorption coefficient, a Gaussian laser beam is used for molecular excitation, and its propagation direction is taken as the *Z*-axis. The beam is focused using a convex lens and the focal point is taken as $z = 0$. The beam has maximum energy density at the focus, which will symmetrically reduce towards either side of it, for the positive and negative values of z. In the experiment, the sample is placed in the beam at different positions with respect to the focus (different values of z), and the corresponding transmission is measured. The sample sees different laser intensity at each position, and hence, its intensity-dependent transmission can be calculated from the position dependent transmission. From this nonlinear transmission information, the nonlinear absorption coefficient can be calculated.

We have used a stepper-motor controlled linear translation stage in our setup to move the sample through the beam in precise steps. The open aperture Z-scan (schematic) experimental set up is shown in Fig. 1. The sample was taken in a 1-mm cuvette. The transmission of the sample at each point was measured by means of two

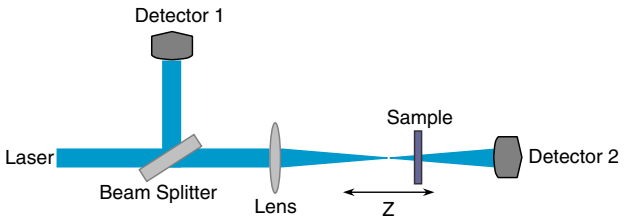

Fig. 1 The open aperture Z-scan schematic

pyroelectric energy probes (Rj7620, Laser Probe Inc.). One energy probe monitored the input energy, while the other monitored the transmitted energy through the sample. The second harmonic output (532 nm) of a Q-switched Nd:YAG laser (Quanta Ray, Spectra Physics) was used for exciting the molecules. The temporal width (FWHM) of the laser pulses is 7 ns. Pulse energy of 16 μJ was used for the experiments. The pulses were fired in the "single shot" mode, allowing sufficient time between successive pulses to avoid accumulative thermal effects in the sample.

DFWM studies

In degenerate four wave mixing (DFWM), four electromagnetic waves of the same optical frequency interact in a nonlinear optical medium through the third-order polarization. The phase-conjugate geometry or the BOXCARS geometry can be used for DFWM experiments. We used the forward folded BOXCARS geometry, where a laser beam is split into three beams, which are aligned such that they form three corners of a square as shown in Fig. 2. The diametrically opposite beams are the pump beams, and they have the same intensity. The third beam is the probe, which has an intensity of about 20% of the pump beam. When the beams are focused onto the sample, the fourth beam (signal beam) is generated due to nonlinear interaction, which will appear on the fourth corner of the square. It can be measured using a photodetector.

Similar to the Z-scan, we used 7-ns laser pulses at 532 nm in our DFWM experiment also. Absorptive-type neutral density filter sets were used to change the intensity of the input laser beam. The sample was taken in a 2-mm path length glass cuvette. The input energy was monitored using a pyroelectric energy probe, and the generated signal beam was measured in the far field using a calibrated photodiode.

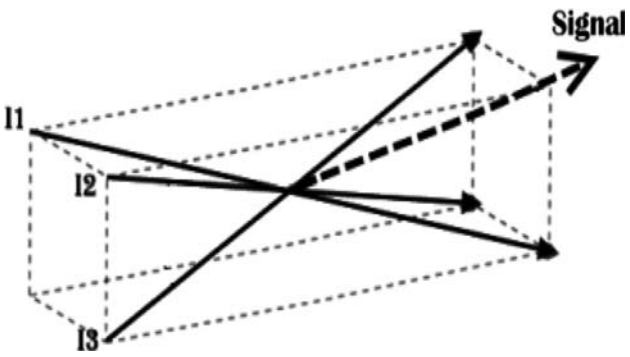

Fig. 2 The BOXCARS geometry for DFWM

*Synthesis of 3,4-diphenylthiophene-2,5-dicarboxylic acid (**2**)*

The 3,4-diphenylthiophene-2,5-dicarboxylic acid (**2**) was synthesized according to the reported procedure [14]. The formation of the required compound was confirmed by its FTIR, mass spectral followed by elemental analyses. Yield: 55%. IR (cm^{-1}), 3450 (br, –OH), 1688 (>C=O). FAB-HRMS: *m*/*z*, 325. Anal. Calcd. for $C_{18}H_{12}N_4O_4S$: C, 66.65; H, 3.73; S, 9.89. Found: C, 66.22; H, 3.88; S, 10.06.

*Synthesis of 3,4-diphenylthiophene-2,5-dicarbonyl chloride (**3**)*

A mixture of 3,4-diphenylthiophene-2,5-dicarboxylic acid (**2**) (0.5 g), 20 mL of thionyl chloride was refluxed for 5 h. The excess thionyl chloride was distilled off and remaining solid residue was extracted with dicloromethane. The solvent was removed by rotary evaporation and the solid product obtained was recrystallized from hexane to yield diacid chloride as white solid. Yield: 70%. IR (cm^{-1}), 1670 (>C=O). Anal. Calcd. for $C_{18}H_{10}Cl_2O_2S$: C, 59.85; H, 2.79; S, 8.88. Found: C, 60.02; H, 2.98; S, 8.66.

*Synthesis of precursor polyhydrazide (**PH1**)*

To a mixture of **1** equivalent of dihydrazide (**4**), two equivalents of anhydrous aluminum chloride and 0.1 mL of pyridine in 50 mL of *N*-methyl pyrrolidone (NMP), one equivalent of diacid chloride (**3**) was added slowly at room temperature. The reaction mixture was stirrer for 5 h at room temperature. Further, it was heated at 80 °C for 20 h. After cooling to room temperature, the reaction mixture was poured into ice cold water and the precipitate separated was collected by filtration. It was washed with water followed by acetone and finally dried in vacuum to get the polyhydrazide (**PH1**). Yield: 76%, IR (KBr, cm^{-1}), 3320 (>N–H), 1725 (>C=O). Anal. Calcd. for $C_{44}H_{56}N_4O_6S_2$: C, 65.97; H, 7.05; N, 6.99; S, 8.01. Found: C, 66.45; H, 7.36; N, 7.28; S, 7.85.

*Synthesis of polymer (**P1**)*

A mixture of polyhydrazide (0.5 g) and 20 mL phosphorus oxychloride was heated at 100 °C for 8 h with stirring. The reaction mixture was then cooled to room temperature and

poured to excess of ice cold water. The resulting precipitate was collected by filtration, washed with water followed by acetone and dried in vacuum oven to get the polymer **P1**. Yield: 82%, ^{1}H NMR (400 MHz, $CDCl_3$). δ(ppm): 7.65–7.18 (m, 10H, phenyl protons), 4.16 (t, 4H. –OCH_2–), 1.98–1.30 (m, 32H, –$(CH_2)_8$–), 0.86 (t, 6H, –CH_3). IR (KBr, cm^{-1}), 1590 (C=N). Anal. Calcd. for $C_{44}H_{52}N_4O_4S_2$: C, 69.08; H, 6.85; N, 7.32; S, 8.38. Found: C, 69.52; H, 6.56; N, 7.48; S, 8.03.

Results and discussion

Synthesis and characterization of the polymer

Scheme 1 outlines the designed synthetic route for the preparation of monomers and the polymer (**P1**). The required 3,4-diphenylthiophene-2,5-dicarboxylic acid (**2**) was synthesized by condensation of 1,2-diphenylethane-1,2-dione (benzil) with diethyl thiodiglycolate (**1**), which was treated with excess thionyl chloride to obtain 3,4-diphenylthiophene-2,5-dicarbonyl chloride (**3**). The 3,4-didecyloxythiophene-2,5-dicarbohydazide (**4**) was synthesized according to the reported procedure [13]. The precursor polyhydrazide (**PH1**) was synthesized by polycondensation of (**4**) with (**3**) in presence of anhydrous aluminum chloride and pyridine. The polyhydrazide was converted into targeted polymer (**P1**) through cyclization using phosphorus oxychloride as dehydrating agent. The structures of newly synthesized compounds were confirmed by their FTIR, ^{1}H NMR, mass spectral, and elemental analyses.

The structure of 3,4-diphenylthiophene-2,5-dicarboxylic acid (**2**) was confirmed by its mass spectrum. Mass spectrum of it showed molecular ion peak at *m/z* 325, which corresponds to its molecular formula $C_{18}H_{12}N_4O_4S$. Formation of precursor polyhydrazide (**PH1**) was evidenced by its FTIR spectral and elemental analyses. The FTIR spectrum of **PH1** exhibited sharp peaks at 3,320 and 1,725 cm^{-1} (Fig. 3) accounting for >N–H and >C=O groups, respectively. The successful conversion of polyhydrazide (**PH1**) into polyoxadiazole (**P1**) was confirmed by FTIR spectrum. In its IR spectrum, disappearance of >C=O and >N–H stretching absorption bands and appearance of a sharp peak at around 1,590 cm^{-1}due to imine of the oxadiazole ring indicate the cyclization (Fig. 3). The chemical structure of the polymer was confirmed by FTIR, ^{1}H-NMR spectroscopy and elemental analysis. FTIR spectrum of **P1** showed characteristic absorption peaks at 2,920, 2,848 cm^{-1} (C–H stretching aliphatic segments), 1,590 cm^{-1} (1,3,4-oxadiazole), 1,467 cm^{-1} (aromatic), 1,060 cm^{-1} (=C–O–C= stretching of oxadiazole). The ^{1}H-NMR spectra of polymer **P1** showed a multiplet at δ 7.18–7.65 ppm, due to the protons of the two phenyl rings on 3- and 4-position of the thiophene unit. Peaks corresponding to the protons of the alkoxy (–OCH_2–) groups at 3- and 4-positions of the thiophene ring appeared at δ 4.16 ppm. A set of multiplet peaks, which corresponds to –CH_2– appeared at δ 1.30–1.98 ppm. The methyl protons (–CH_3) of the alkoxy substitution resonated as a triplet at δ 0.86 ppm. The elemental analysis results of these polymers were in agreement with their expected empirical formula. The weight average molecular weight of the polymer (THF soluble part) was determined to be 4,870 g/mol, which clearly confirms its polymeric nature. The molecular weight and polydispersity data of the polymer **P1** are summarized in Table 1.

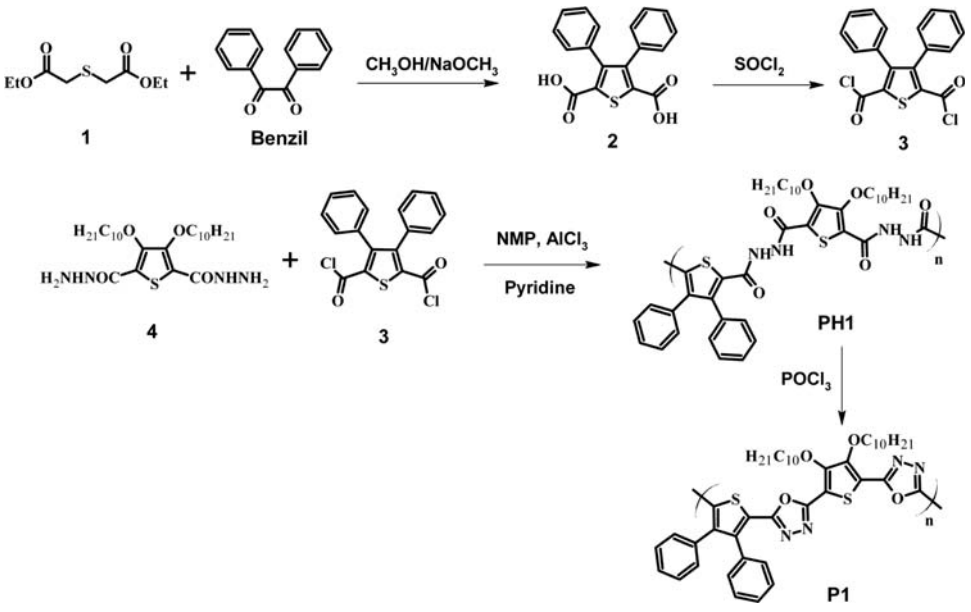

Scheme 1 Designed scheme for the preparation of polymer

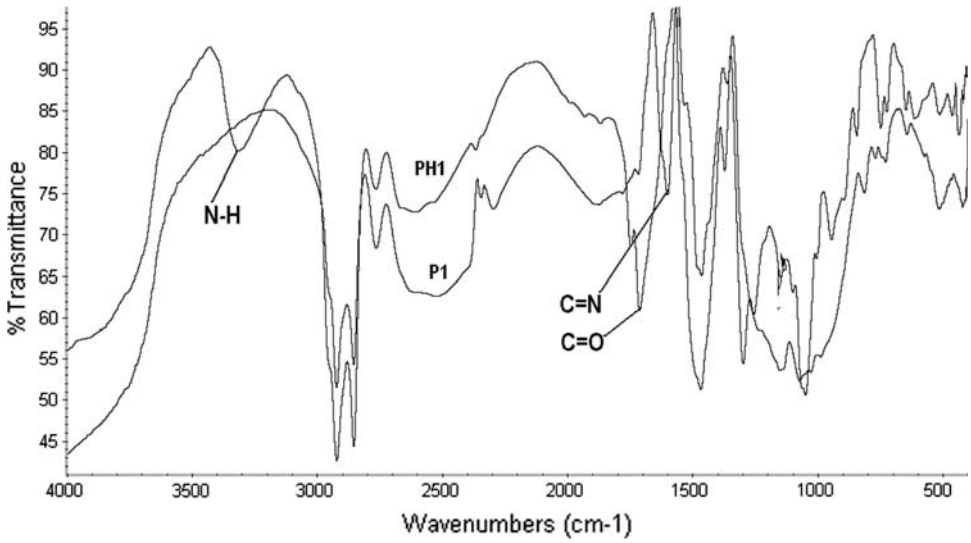

Fig. 3 FTIR spectra of polyhydrazide (**PH1**) and polymer (**P1**)

Table 1 The molecular weight data, electrochemical potentials, and energy levels of the polymer **P1**

Polymer	M_n^a	M_w^b	PD[c]	E_{oxd} (onset)	E_{red} (onset)	E_{oxd}	E_{red}	HOMO (eV)	LUMO (eV)	E_g (eV)
P1	3150	4870	1.55	1.50	–0.70	2.05	–1.80	–5.84	–3.64	2.20

[a] Number average molecular weight

[b] Weight average molecular weight

[c] Polydispersity

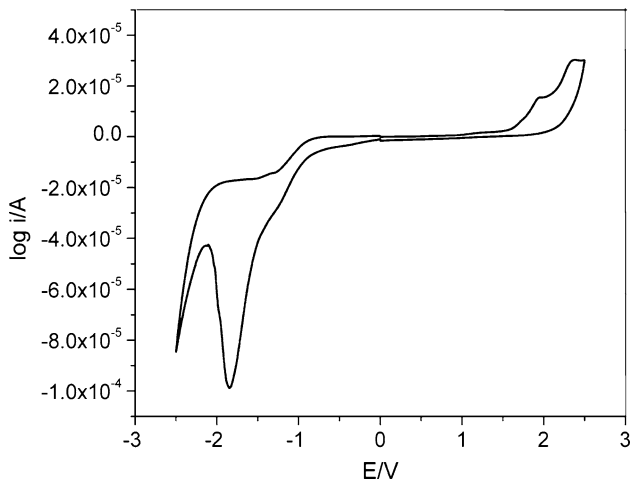

Fig. 4 Oxidation and reduction cyclic voltammetric waves of the polymer

Thermogravimetric analysis of the polymer was carried out under nitrogen atmosphere at heating rate of 10 °C/min. The polymer is found to be thermally stable up to 300 °C.

Redox properties of the polymer

Cyclic voltammetry (CV) was employed to determine redox potentials of new polymer and then to estimate the HOMO and LUMO energy of the polymer, which is of importance to determine the band gap. The cyclic voltammogram of the polymer coated on a glassy carbon electrode was measured on AUTOLAB PGSTAT 30 electrochemical analyzer, using a Pt counter electrode and a Ag/Ag^+ reference electrode, immersed in the electrolyte [0.1 M $(n\text{-Bu})_4NClO_4$ in acetonitrile] at a scan rate of 25 mV/s. Electrochemical data of the polymer is summarized in Table 1.

While sweeping cathodically (Fig. 4), the polymer showed reduction peak at −1.80 V. These reduction potentials are lower than those of 2-(4-biphenyl)-5-(4-terbutylphenyl)-1,3,4-oxadiazole (PBD) [16, 17], one of the most widely used electron transporting material. In the anodic sweep (Fig. 4), polymer showed oxidation peak at 2.05 V with an onset oxidation potential 1.50 eV. The onset potentials of *n*- and *p*-doping processes can be used to estimate the HOMO and LUMO of the polymer. According to the equations reported in the articles [18–20], $E_{HOMO} = -\left[E_{onset}^{oxd} + 4.4\,eV\right]$ and $E_{LUMO} = -\left[E_{onset}^{red} - 4.4\,eV\right]$ where E_{onset}^{oxd} and E_{oxd}^{red} are the onset potentials versus SCE for the oxidation and reduction of the polymer.

The HOMO energy level of the polymer was estimated to be −5.84 eV, which is comparable with CN-PPV. The LUMO energy level (−3.64 eV) is lower then those of PPV and some other *p*-type conjugated polymers indicating the polymer is having better electron transporting property. The very high electron affinity of this polymer is due to the

incorporation of electron deficient oxadiazole ring in the polymer backbone. From the onset potentials of oxidation and reduction process, the band gap of the polymer is estimated to be 2.2 eV.

Optical characterization

Linear optical properties

The UV–visible absorption spectrum of the polymer **P1** was recorded both in solution and in thin film forms. As shown in Fig. 5, the absorption maximum of the polymer in dilute $CHCl_3$ solution is at 392 nm. The absorption spectrum of the polymer in thin film (Fig. 5) shows 28 nm bathochromic shift, indicating the presence of inter-chain interactions in the solid state. Their optical band gap (E_g) calculated from the absorption edge of the spectrum was found to be 2.27 eV. The value is quite close to that obtained by the electrochemical method.

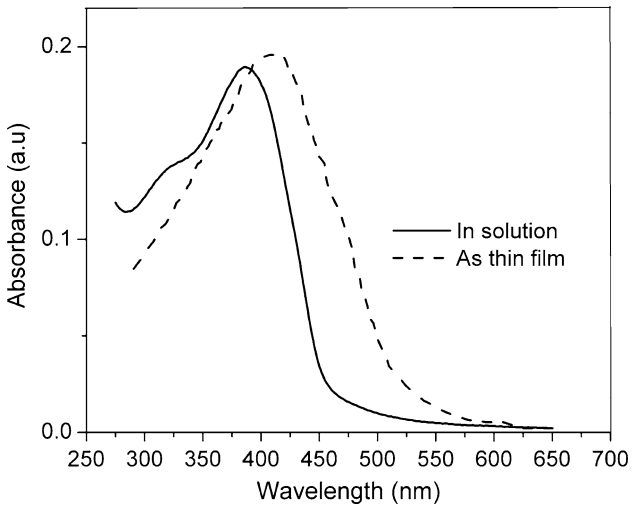

Fig. 5 UV–vis absorption spectrum of the polymer in solution and thin film form

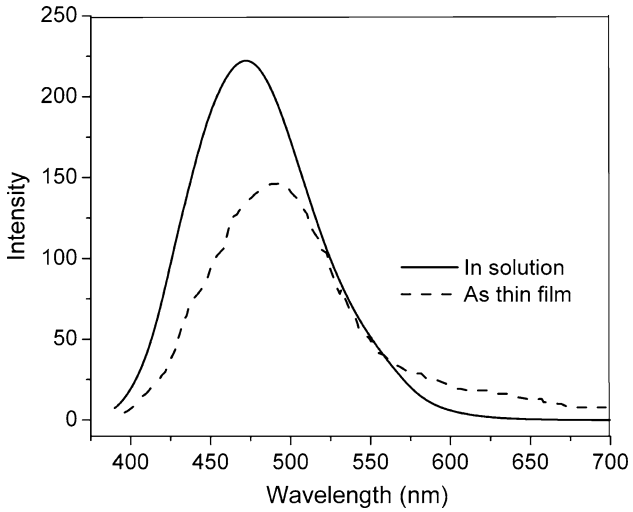

Fig. 6 Fluorescence emission spectra of polymer in solution and thin film form

As shown in Fig. 6, the emissive maximum (excitation wavelength 370 nm) of the polymer in dilute $CHCl_3$ solution is at 472 nm. The fluorescence emission spectrum of the polymer in thin film (Fig. 6) shows red shift (26 nm) with respect to those obtained from their solution. The polymer emits intense bluish-green fluorescence in solid state with the emission peak at 498 nm. The Stokes shift is found to be 78 nm. The fluorescence quantum yield of the polymer in solution is determined to be 35% against quinine sulfate as a standard (10^{-5} M quinine sulfate in 0.1 M H_2SO_4). These results clearly indicate that the newly synthesized polymer **P1** is a promising material for applications in opto-electronic devices. The device fabrication and their characterization are in progress.

Nonlinear optical properties

Z-scan The absorption spectrum of the polymer in dilute $CHCl_3$ solution shows that the excitation wavelength of 532 nm is close to the long-wavelength absorption edge. The linear absorption coefficient (α) for the polymer at 532 nm is given in Table 2. When taken in a 1-mm cuvette, the sample has a linear transmission of 83% for the same concentration of the polymer at 532 nm. As shown in Fig. 7, this sample shows strong optical limiting behavior, as the transmittance decreases when the pump intensity is increased. It is seen that a three-photon absorption (3PA) type process gives the best fit to the obtained experimental data. The intensity versus normalized transmission curves derived from the Z-scan data are, therefore, numerically fitted to the nonlinear transmission equation for a three-photon absorption process, given by the Eq. 1:

$$T = \frac{(1-R)^2 \exp(-\alpha L)}{\sqrt{\pi} p_0} \int_{-\infty}^{+\infty} \ln\left[\sqrt{1 + p_0^2 \exp(-2t^2)} + p_0 \exp(-t^2)\right] \mathrm{d}t \quad (1)$$

where T is the transmission of the sample, R the Fresnel reflection coefficient at the sample–air interface, α the absorption coefficient, and L the sample length. p_0 is given by $[2\gamma(1-R)^2 I_0^2 L_{\mathrm{eff}}]^{1/2}$ where γ is the three-photon absorption coefficient, and I_0 is the incident intensity. L_{eff} is given by $[1-\exp(-2\alpha L)]/2\alpha$. The 3PA coefficient obtained from the curve fitting is tabulated in Table 2. While doing the calculation, the pulse-to-pulse energy fluctuations of the laser also are taken into account, and hence the simulated curve is not fully smooth.

Table 2 Linear and nonlinear optical parameters for the polymer

Linear optical properties			Z-scan	DFWM			
Sample	n_0^a	α^b (m^{-1})	γ (10^{-22} m^3/W^2)	$\chi^{(3)}$		F	
				(10^{-20} m^2/V^2)	(10^{-12} esu)	(10^{-23} m/V^2)	(10^{-13} esu)
P1	1.4445	164.25	5.0	1.157	0.831	7.04	5.06

[a] Refractive index

[b] Absorption coefficient

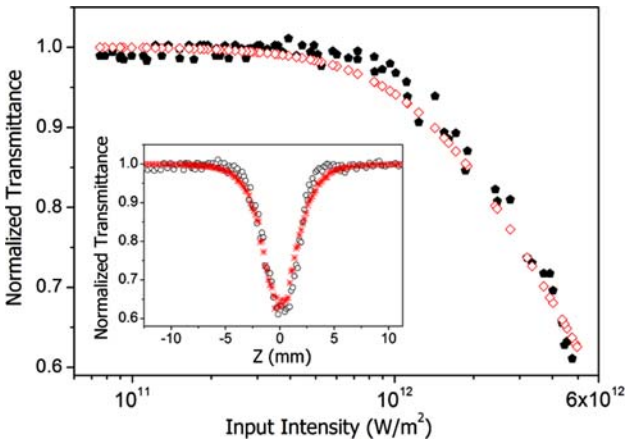

Fig. 7 Input intensity versus normalized transmittance for the polymer. *Inset* shows the Z-scan curve. *Filled circles* show the data points and the *hollow squares* give the best 3PA fit to the data

Considering the absorption spectra of the samples and recalling that pure three-photon absorption cross-sections are generally very low, it seems that the observed nonlinearity arises from sequential three-photon absorption involving excited states. Two-photon absorption followed by excited state absorption is another possibility. Therefore, the nonlinearity can be considered as an "effective" three-photon absorption process. In a pure 3PA process, three photons will be simultaneously absorbed and this is an instantaneous nonlinear optical phenomenon. Compared to the usual one-photon absorption process, the cross section for a 3PA is generally low, but they become significant when the samples are irradiated with intense laser pulses of picoseconds or shorter duration. With nanosecond pulse excitation, accumulative nonlinear optical phenomena like excited state absorption and free carrier absorption become more prominent. Depending on the material system under study, excitation wavelength and applied laser fluence, a combination of the instantaneous and accumulative nonlinear effects may take place. These, however, will appear like pure 2PA or pure 3PA in a simple transmission measurement like the Z-scan. These combined nonlinearities can hence be termed as "effective 2PA" and "effective 3PA" processes to distinguish them from pure 2PA and 3PA processes. Such absorptive nonlinearities involving real excited states have been reported earlier in C_{60}, semiconductors, metal nanoclusters, phthalocyanines, and some fluorine derivatives [21–26]. During the 3PA process, excitation is proportional to the cube of the incident intensity. This feature may help to obtain higher contrast and resolution in imaging, as 3PA provides a stronger spatial confinement. With the availability of ultrafast pulsed lasers in recent years, significant progress in 3PA-based applications has been witnessed including three-photon pumped lasing and 3PA based optical limiting and stabilization [27].

In π-conjugated polymeric systems, electrons can move in large molecular orbitals which result from the linear superposition of the carbon p_z atomic orbitals, leading to a very high optical nonlinearity, which increases with the conjugation length [28]. The polymer studied in the present work consists of thiophene ring substituted with dodecyloxy pendant at 3,4-position as electron donating group and 1,3,4-oxadiazole along with 3,4-diphenylthiophene moieties as electron withdrawing groups. This leads to formation of a donor–acceptor type of arrangement in the polymer backbone. The enhanced third-order nonlinearity in the polymer arises due to the high π-electron density along the polymeric chain, which are easily polarizable as a result of the alternating donor–acceptor type of arrangements. Further, increased conjugation due to phenyl substitution on thiophene ring also enhances the NLO property.

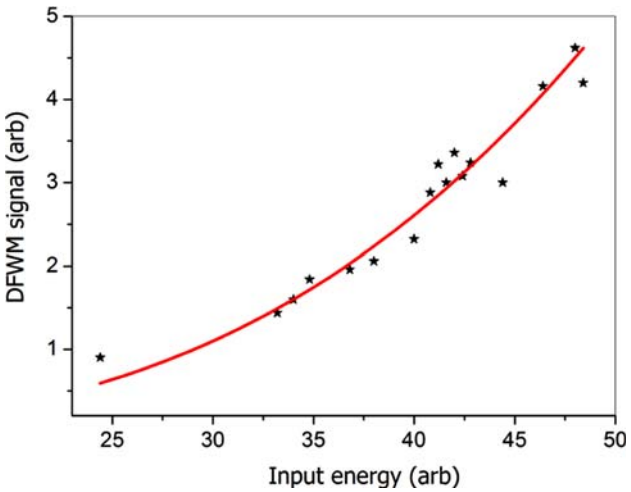

Fig. 8 DFWM signal versus input laser energy for CS_2

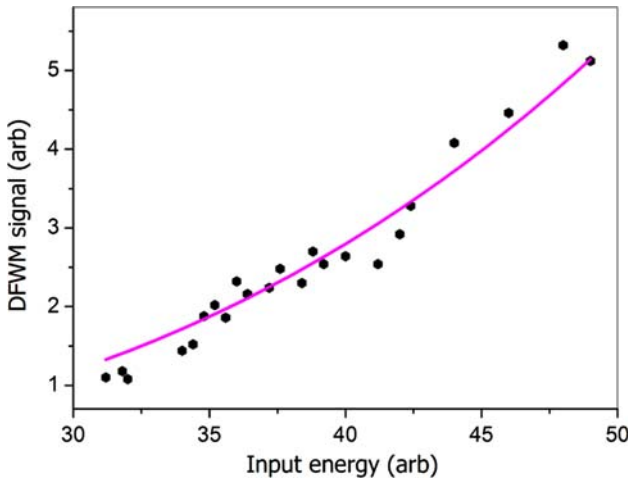

Fig. 9 DFWM signal versus input laser energy for the polymer

DFWM Figure 8 shows the variation of the DFWM signal in the reference sample CS_2 as a function of the pump intensity. The DFWM signal obtained for the polymer is shown in Fig. 9. The signals are proportional to the cubic power of the input intensity as given by the equation,

$$I(\omega)\alpha\left(\frac{\omega}{2\varepsilon_O cn^2}\right)\left|\chi^{(3)}\right|^2 l^2 I_0^3(\omega) \quad (2)$$

where $I(\omega)$ is the DFWM signal intensity, $I_o(\omega)$ the pump intensity, l the length of the sample, and n the refractive index of the medium. The solid curves in the figures are cubic fits to the experimental data. The third-order susceptibility $\chi^{(3)}$ of the sample can be calculated from the fits using the equation,

$$\chi^{(3)} = \chi_R^{(3)}\left[\frac{(I/I_0^3)}{(I/I_0^3)_R}\right]^{1/2}\left[\frac{n}{n_R}\right]^2\frac{l_R}{l}\left(\frac{\alpha l}{(1-e^{-\alpha l})e^{-\alpha l/2}}\right) \quad (3)$$

where the subscript 'R' refers to the standard reference, CS_2. '$\chi_R^{(3)}$' is taken to be 9.5×10^{-21} m^2/V^2 [15]. The figure of merit F, given by $\chi^{(3)}/\alpha$ is then calculated. F is a measure of nonlinear response that can be achieved for a given absorption loss in the medium. The F value is useful for comparing the nonlinearity of different materials when excited in spectral regions of non-zero absorption. Table 2 shows that the polymers have good F values. The $\chi^{(3)}$ and F values are given in both cgs and SI units.

Conclusions

In conclusion, a new conjugated polymer (**P1**) carrying 2-(3,4-didecyloxythiophen-2-yl)-5-[3,4-diphenyl-5-(1,3,4-oxadiazol-2-yl)thiophen-2-yl]-1,3,4-oxadiazole as repetitive unit with donor and acceptor moieties in the molecular architecture has been successfully synthesized through multistep reactions. The newly synthesized compounds have been characterized by different spectroscopic techniques. The electrochemical properties showed that the polymer possesses high-lying HOMO energy level (−5.84 eV) and low-lying LUMO energy level (−3.64 eV). This is attributed to the presence of alternate donor–acceptor conjugated units along the polymer backbone. The linear optical properties revealed that the polymer emits bluish-green fluorescence under the irradiation of light. The fluorescence quantum yield of the polymer in solution is determined to be 35%. The nonlinear optical properties of the polymer have been studied using the Z-scan and DFWM techniques. The polymer exhibited effective 3PA. Values of the three-photon absorption coefficients (γ), third-order nonlinear susceptibilities ($\chi^{(3)}$), and figures of merit (F) have been calculated. The absorptive nonlinearity observed is of the optical limiting type, which can have potential applications. The studies reveal that the new polymer **P1** is a promising material for the development of efficient photonic devices.

Acknowledgements The authors are grateful to the CDRI, Lucknow, NMR research centre, IISc Bangalore, and RRL, Trivandrum, for providing instrumental analyses.

References

1. Sutherland RL (1996) Handbook of nonlinear optics. Dekker, New York
2. Perry JW, Mansour K, Lee I-YS, Wu X-L, Bedworth PV, Chen C-T, Ng D, Marder SR, Miles P, Wada T, Tian M, Sasabe H (1996) Science 273:1533
3. Ronchi A, Cassano T, Tommasi R, Babudri F, Cardone A, Farinola GM, Naso F (2003) Synth Met 139:831
4. Cassano T, Tommasi R, Babudri F, Cardone A, Farinola GM, Naso F (2002) Opt Lett 27:176
5. Burroughes JH, Bradley DDC, Brown AR, Marks RN, Mackay K, Friend R, Burn PL, Holmes AB (1990) Nature 347:539
6. Grem G, Leditzky G, Ullrich B, Leising G (1992) Adv Mater 4:36
7. Leclerc M (2001) J Polym Sci Part A: Polym Chem 39:2867
8. Pei J, Yu W-L, Haung W, Heeger AJ (2000) Chem Commun 1631
9. Nisoli M, Cybo-Ottone A, De Silvestri S, Magni V, Tubino R, Botta C, Musco A (1993) Phys Rev B 147:10881
10. Roncali J (1992) Chem Rev 92:711
11. Kishino S, Ueno Y, Ochiai K, Rikukawa M, Sanui K, Kobayashi T, Kunugita H, Ema K (1998) Phys Rev B 58:R13430
12. John Kiran A, Udayakumar D, Chandrasekharan K, Adhikari AV, Shashikala HD (2006) J Phys B: Mol Opt Phys 39:3747
13. Udayakumar D, Adhikari AV (2006) Synth Met 156:1168
14. Henckens A, Colladet K, Fourier S, Cleij TJ, Lutsen L, Gelan J, Vanderzande D (2005) Macromolecules 38:19
15. Sheik-Bahae M, Said AA, Wei T, Hagan DJ, Van Styrland EW (1990) IEEE J Quantum Electron 26:760
16. Strukelj M, Papadimitrakopoulos F, Miller TM, Rotheberg LJ (1995) Science 267:1969
17. Janietz S, Wedel A (1997) Adv Mater 9:403
18. de Leeuw DM, Simenon MMJ, Brown AB, Einerhand REF (1997) Synth Met 87:53

19. Agrawal AK, Jenekhe SA (1996) Chem Mater 8:579
20. Yang C-J, Jenekhe SA (1995) Macromolecules 28:1180
21. Harilal SS, Bindhu CV, Nampoori VPN, Vallabhan CPG (1999) J Appl Phys 86:1388
22. Tutt LW, Boggess TF (1993) Progr Quantum Electron 17:299
23. Philip R, Ravindrakumar G, Sandhyarani N, Pradeep T (2000) Phys Rev B 62:13160
24. Santosh Kumar RS, Venugopal Rao S, Giribabu L, Narayana Rao D (2007) Chem Phys Lett 447:274
25. Cohanoschi I, Garcı M, Toro C, Belfield KD, Hernandez FE (2006) Chem Phys Lett 430:133
26. Wang P, Ming H, Xie J, Zhang W, Gao X, Xu Z, Wei X (2001) Opt Comm 192:387
27. Zheng Q, He GS, Lu C, Prasad PN (2005) J Mat Chem 15:3488
28. Cassano T, Tommasi R, Tassara M, Babudri F, Cardone A, Farinola GM, Naso F (2001) Chem Phys 272:111